

Optimal Sizing of PMSG for Wind Turbine Applications: Methodology and Analysis

The - Cong Nguyen and Thanh - Khang Nguyen
 Hanoi University of Science and Technology, Hanoi, Vietnam
 Email: {cong.nguyenthe, khang.nguyenthanh}@hust.edu.vn

Duc - Hoan Tran
 Altran Technology, Toulouse, France
 Email: tduchoan@gmail.com

Abstract—This papers describes the methodology to optimal design of the Permanent Magnet Synchronous Generator (PMSG) of wind turbine systems at the low average wind speed. In order to reduce the loss on systems and the robustness of optimal methodology, the authors used the algorithm genetic for optimization process, the method results will be analysis for characterization of control in order of protection and implementation for the wind turbine system with the power of 15- 20 kW at 6m/s average wind speed. To step up the efficiency of optimal methodology, the authors proposed the concept of PMSG for the “passive” wind turbine systems (without the control MPPT by power electronic inverter) and using the diodes rectifier for the system design and optimization process. Sample simulation results for three optimal Permanent Magnet Synchronous Generators have been presented and discussed for the fundamental issues.

Index Terms—passive wind turbine systems, permanent magnet synchronous generator (PMSG), optimization, genetic algorithm, NSGA-II

I. INTRODUCTION

Wind turbines can be made with either constant-speed or variable-speed in term of mechanical input speed, one of the areas where technological advances have played a major role in the last years is the development of innovative variable-speed wind turbines. The variable-speed wind turbine has several advantages, like higher energy extraction from the wind [1], lower noise at low wind speed and cleaner power transfer to grid [2], [3]. For these reasons, the variable-wind speed is taking an increasing share of the market nowadays.

The investigation of aerodynamic generators with minimal mass and cost of active material requires an overview of the various concepts. The PMSG type is well established among them by the high efficiency and reducible mass. However, extracting as much power as possible from low wind speed and minimization weight, while obtaining a suitable dc-link voltage $V_{dc} = 600V$ is the key to realize this study.

The authors have developed an optimal methodology base on the design of “passive” wind turbine system show in Fig. 1 as the solution to realize the above objectives.

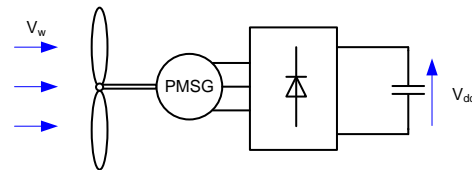


Figure 1. “Passive” wind turbine system

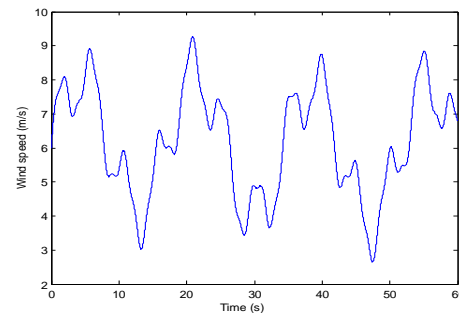


Figure 2. Wind speed profile

II. MODELING OF “PASSIVE” WIND TURBINE SYSTEM

A. Wind Model

The average wind speed depends on the region and on the season, for this study, the authors proposed the concept of system with the low average wind speed. In order to robustness modeling, the wind speed have to variation in interval sufficient large. Thus, the stochastic model of wind speed by decomposing a discrete Fourier transformation with 6m/s average value is used in this study [4]. The wind speed so that expressed as the function of time:

$$V_w(t) = 6 + 0.2\sin(0.1047t) + 2\sin(0.2665t) + \sin(1.2930t) + 0.2\sin(3.6645t) \quad (1)$$

B. Modeling of Wind Turbine

The conversion efficiency of the system from wind power to electrical power is given by the product of the

power coefficient C_p [5], alternator efficiency and power-electronic converter efficiency. Overall efficiency is defined as the average conversion from energy available in the wind to produced electrical energy. Then the wind turbine can be modeled by static and dynamic model.

1) *Static model*: The mechanical power and the torque developed by a wind turbine rotor vary according to the equation:

$$P_w = \frac{1}{2} \rho C_p(\lambda) \pi R_w^2 V_w^3 \quad (2)$$

$$T_w = \frac{P_w}{\Omega_w} = \frac{1}{2} \rho C_p(\lambda) \pi \frac{R_w^2 V_w^3}{\Omega_w} \quad (3)$$

where

R_w , blade radius of wind turbine [m]

ρ air density [kg/m^3]

T_w , mechanical torque from wind blades [N.m]

Ω_w , rotational speed [rad/s]

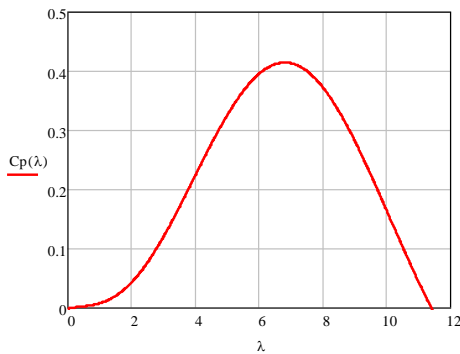


Figure 3. Power coefficient of wind turbine

The type of wind turbine in this work is the three-bladed with the radius $R_w=10\text{m}$ and the power coefficient C_p may be expressed as a function of the tip speed ratio $\lambda = R_w \Omega_w / V_w$, given by equation (4) and shows on Fig. 3:

$$\begin{aligned} A0 &:= -1.53 \cdot 10^{-3} & A1 &:= 1.34 \cdot 10^{-2} & A2 &:= -1.76 \cdot 10^{-2} \\ A3 &:= 1.64 \cdot 10^{-2} & A4 &:= -3.1 \cdot 10^{-3} & A5 &:= 2.1 \cdot 10^{-4} \\ A6 &:= -4.21 \cdot 10^{-6} & A7 &:= -3.98 \cdot 10^{-8} \end{aligned}$$

$$C_p(\lambda) := A7 \cdot \lambda^7 + A6 \cdot \lambda^6 + A5 \cdot \lambda^5 + A4 \cdot \lambda^4 + A3 \cdot \lambda^3 + A2 \cdot \lambda^2 + A1 \cdot \lambda + A0 \quad (4)$$

2) *Dynamic model*: The dynamic equation for interaction between turbine-PMSG is written by equation of torque:

$$T_w - T_{em} = J_w \frac{d\Omega_w}{dt} + f_w \Omega_w \quad (5)$$

where: T_w , T_{em} are respectively the wind turbine mechanical torque (3) and PMSG electromagnetic torque.

J_w and f_w being the total wind turbine inertia and viscous friction coefficient. Typically, in this work, the authors fix the values of $J_w = 5.5 \text{ N.m}^2$ and $f_w = 0.5 \text{ N.m.s/rad}$.

When wind speed changes on the function of time, the rotational speed should be adjusted to achieve the maximum value of C_p , the control strategy to achieve the maximum value of C_p is called MPPT (Maximal Power

Point Tracking). Generally, the MPPT control of wind turbine is taken by power electronic converter.

C. Analytical Modeling of PMSG

In order of optimization the PMSG for wind turbine system integrated with wind speed profile, wind turbine and diode rectifier. The authors will present the analytical model of PMSG in this section.

In PMSG, the excitation is provided by permanent magnets instead of field winding. Permanent magnet machines are characterized as having large air gaps, which reduce flux linkage even in machines with multi magnetic poles [6]-[7].

As the result of previous study [8]-[9], low rotational speed generators can be manufactured with relatively small sizes with respect to its power rating. Moreover, gearbox can be omitted due to low rotational speed in PMSG wind generation system, resulting in low cost. In a recent survey, gearbox is found to be the most critical component, since its downtime per failure is high in comparison to other components in the wind turbine system.

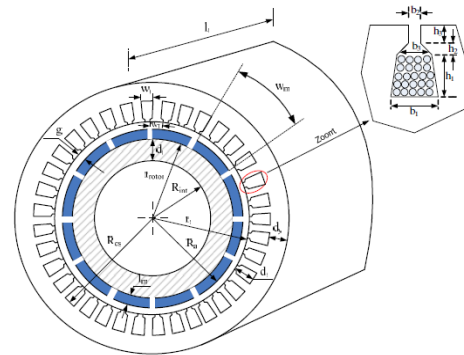


Figure 4. PMSG topology

TABLE I. GEOMETRICAL AND BASIC DESIGN PARAMETERS

PMSG Geometrical parameters		PMSG basic design variables	
r_s	Bore radius	R_t	Bore radius/length ratio
g	Air gap	R_{dr}	Slot depth/ bore radius ratio
l_r	Length active	J_s	Current density
d_s	Slot depth	B_y	Yoke induction
w_s	Slot width	P_b	Power at the base functional point
w_T	Tooth width	p	Number of pole pair
d_r	Rotor yoke thickness	N_{spp}	Number of slots per pole and phase
d_y	Stator yoke thickness	Ω_b	Base speed

The most important in the design PMSG model is the variables chosen have to be independent. Thus, the sizing model of PMSG in this work has been developed in [10]. This model depends on geometrical characteristics and electromagnetic characteristics, the 8 basic design variables for the sizing PMSG model is presented on Table I. The electromagnetic and geometrical parameters of PMSG should calculate from these 8 basic variables.

The geometrical characteristics of PMSG are illustrated on Fig. 4. With this topology, we have to define the 8 geometrical fundamental dimensions on Table I.

3) Sizing of geometrical parameters

The bore radius r_s is related to the fundamental value of the air gap magnetic flux density (B_{1g}) and to the slot depth / bore radius ratio R_{dr} ($R_{dr} = d_s/r_s$) as follows:

$$r_s = \left(T_b R_{rl} \frac{1}{J_s K_r B_{1g} R_{dr} \pi} \right)^{\frac{1}{4}} \quad (6)$$

where K_r is the slot filling coefficient, B_{1g} is computed from the magnet properties (relative permeability $\mu_r = 1.05$ and remanent induction $B_r = 1.1$ T for Nd-Fe-B magnet) and from the electrical half pole width α_m :

$$B_{1g} = \frac{4}{\pi} B_r \frac{l_m / g'}{\mu_r + (l_m / g')} \sin(\alpha_m) \quad (7)$$

where $l_m / g' = l_m / (K_C g)$ represents the ratio between the magnet thickness and the air gap corrected by the Carter coefficient. In these two equations (6) and (7), the unknown variables are set to typical values: $K_r = 0.35$, $\alpha_m \approx 1.31$ (i.e. 75°) and $l_m / g' = 3.5$ and the Carter coefficient K_C is set to 1.05 in this work.

The magnet width w_m can be deduced as follows:

$$w_m = \frac{r_s \alpha_m}{p} \quad (8)$$

The generator air gap g is calculated from the empiric relation:

$$g = 0.001 + 0.003 r_s / \sqrt{R_{rl}} \quad (9)$$

Tooth and slot widths are then obtained from the bore radius and the number of slots per pole per phase N_{spp} :

$$w_s = w_T = \frac{\pi r_s}{6 p N_{spp}} \quad (10)$$

And the slot depth d_s is given by:

$$d_s = R_{dr} r_s \quad (11)$$

Finally, the yoke thickness of rotor and stator ($d_y = d_r$) is obtained as follows:

$$d_y = \frac{r_s}{p} \alpha_m \frac{\hat{B}_g}{\hat{B}_y} \quad (12)$$

where the maximum magnetic flux density in the air gap is evaluated from the following relation:

$$\hat{B}_g = B_r \frac{l_m / g'}{\mu_r + l_m / g'} \quad (13)$$

In order to calculate the output power of the generator, the inductance and resistance of the armature winding must be known. In the calculation of the tooth tip leakage inductance and magnetizing inductance, the permanent magnets are assumed to have the same permeability as air.

4) Calculation of electrical parameters

The main inductance L_m can be calculated as:

$$L_m = \frac{4 \mu_0 l_r r_s}{\pi (K_C g + l_m / \mu_r)} K_b^2 N_{spp}^2 N_{cs}^2 \quad (14)$$

N_{cs} is the number of conductors per slots.

The slot leakage inductance can be computed as

$$L_l = 2 \mu_0 l_r p N_{spp} \lambda_{sl} N_{cs}^2 \quad (15)$$

where λ_{sl} is the specific permeance of the slot leakage.

For the proposed generator type, with equal current in the upper and lower conductor in the slots, the average specific permeance of the slot leakage for the one coil side in the slot can be expressed as

$$\lambda_{sl} = \frac{2h_1}{3(b_1 + b_3)} + \frac{2h_2}{b_2 + b_3} + \frac{h_3}{b_2} \quad (16)$$

The corresponding stator inductance L_s is given by the following relation:

$$L_s = \frac{3}{2} L_m + L_l \quad (17)$$

A typical value of the stator per phase resistance at rate load and average ambient temperature is:

$$R_s = \frac{2 p N_{spp} (l_r + l_e) \cdot \frac{N_{cs}^2}{S_{slot}}}{\sigma_{cu}} \quad (18)$$

Where σ_{cu} is the conductivity of copper, $l_e = \pi(r_s + 0.5d_s)/p$ is the end winding and $S_{slot} = 0.5 \cdot K_r \cdot h_l \cdot (b_1 + b_3)$ is the efficient section of one slot.

The magnetic flux is approximated by

$$\Phi_s = 2 K_b N_{spp} B_{1a} r_s l_r N_{cs} \quad (19)$$

D. Volum and Mass of PMSG

The PMSG masses are obtained from the volume of each constitutive element and its corresponding mass density. The PMSG rotor mass is given by:

$$M_{rotor} = V_{ironrotor} \rho_{iron} + V_{magnets} \rho_{magnet} \quad (21)$$

With the $\rho_{iron} = 7800 \text{ kg} \cdot \text{m}^{-3}$ and $\rho_{magnet} = 7400 \text{ kg} \cdot \text{m}^{-3}$, the volume V_{iron} and $V_{magnets}$ are calculated by:

$$V_{rotor} = \pi l_r (r_{rotor}^2 - (r_{rotor} - d_r)^2) \quad (22)$$

$$V_{magnet} = \pi l_r p K_p \left((r_s - g)^2 - r_{rotor}^2 \right) \quad (23)$$

The stator volume V_{stator} is composed of yoke and teeth volumes:

$$V_{stator} = V_{teeth} + V_{yoke} \quad (24)$$

Which the volume of yoke and teeth can be approximated as follows:

$$\begin{cases} V_{yoke} = 2 \pi l_r d_y (r_s + d_s + d_y / 2) \\ V_{teeth} = \pi l_r d_s (r_s + d_s / 2) \end{cases} \quad (25)$$

The corresponding mass is

$$M_{stator} = V_{stator} \rho_{iron} \quad (26)$$

Finally, the mass of the generator can be expressed by summing stator and rotor masses:

$$M_{PMSG} = M_{stator} + M_{rotor} \quad (27)$$

E. Modeling of PMSG and Diode Rectifier Circuit

The average of output voltage V_{dc} and current I_{dc} (i.e Fig. 5) expression can be expressed in terms of the rms

value of phase voltage and current (fundamental component) of the generator as following:

$$V_{dc} = \frac{3\sqrt{6}}{\pi} \cdot V_{sms} \quad (28)$$

$$I_{dc} = \frac{\pi}{\sqrt{6}} \cdot I_{sms} \quad (29)$$

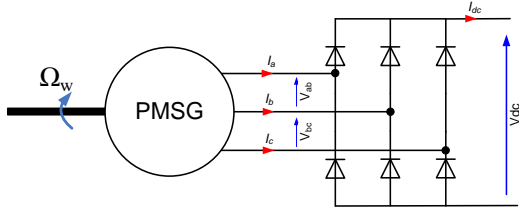


Figure 5. PMSG and diode rectifier

Using the equations (28) and (29) with the value of $V_{dc} = 600V$, we can calculate the rms value of PMSG phase voltage and the PMSG current is computed by current density J_s and section of conductor $S_{cond} = S_{slot}/N_{cs}$.

F. Modeling of Loss and Power Summation

In the losses model of wind turbine and PMSG, we have examined the mechanic loss in turbine, copper loss and iron loss in the PMSG.

Mechanic losses in the turbine:

$$P_{mec} = f_w \Omega_w^2 \quad (30)$$

The copper losses of PMSG at a winding can be calculated from the resistance equivalent R_{dc} and the current equivalent I_{dc} :

$$P_j = 3R_s I_s^2 \quad (31)$$

The core losses of PMSG have to be calculated for each part of the iron core because the difference of induction for each region into stator of PMSG. The authors divide by iron losses in yoke and teeth. The iron losses of each component are caused by hysteresis losses and eddy current losses, calculated as follows:

$$\begin{cases} P_{Hyst}^{yoke} = V_{yoke} \frac{2K_H}{\pi} \hat{B}_y^2 \omega \\ P_{Eddy}^{yoke} = V_{yoke} \frac{4\alpha_p}{\pi^2 K_p} \hat{B}_y^2 \omega^2 \end{cases} \quad (32)$$

where the filling coefficient K_p equals 0.833 and where K_H and α_p are empiric factors depending on the material (typically $K_H = 52$ and $\alpha_p = 0.06$ for FeSi 3%). Similarly, iron losses in the teethes can be deduced by the following relation

$$\begin{cases} P_{Hyst}^{teeth} = V_{teeth} \frac{2K_H}{\pi} \hat{B}_{teeth}^2 \omega \\ P_{Eddy}^{teeth} = V_{teeth} \frac{12\alpha_p N_{spp}}{\pi^2} \hat{B}_{teeth}^2 \omega^2 \end{cases} \quad (33)$$

$$\text{with} \quad \hat{B}_{teeth} = \frac{\hat{B}_g}{0.5 + \frac{d_s}{3r_s}} \quad (34)$$

Therefore, the total core losses in the PMSG is

$$P_{fer} = P_{hys}^{yoke} + P_{edd}^{yoke} + P_{hys}^{teeth} + P_{edd}^{teeth} \quad (35)$$

Finally, the output power of system is calculated by:

$$P_{useful} = P_{wind} - P_{mec} - P_{fer} - P_j \quad (36)$$

G. PMSG Thermal Model

The proposed thermal model of PMSG in this paper is based on the lumped-parameter network of thermal resistances [11]-[12], the temperatures are calculated on slot copper T_{bob} , slot insulation T_{iso} , stator yoke T_{co} , carter T_{ca} by using the ambient air is the referential temperature as Fig. 6.

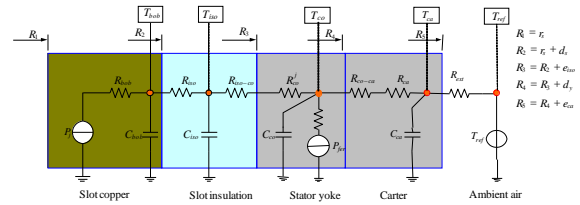


Figure 6. Thermal model of PMSG

The heat transfer modes considered are the conduction and convection modes. The thermal horizontal mode is neglected because the relatively low temperature difference between the generators parts. Finally, the temperatures in the all regions of PMSG are found from differential equations:

$$\dot{T} = AT + Bu \quad (37)$$

With $T = [T_{bob} \ T_{iso} \ T_{co} \ T_{ca}]^T$ and the calculation of matrix A and B is presented in [13], the elements of these matrix depend on geometrical and characteristic material of PMSG and $u = [P_j \ P_{fer} \ T_{ref}]^T$. Nevertheless, in steady-state, the vector T of temperature is calculated by:

$$T = A^{-1}Bu \quad (38)$$

III. OPTIMIZATION OF "PASSIVE" SYSTEM BY GENETIC ALGORITHM

A. Algorithm of Optimization

Multi-objective optimization method seeks simultaneously to minimize N objectives where each of them is a function of a vector X of m parameters (decision variables or design variables) [14]. These parameters may also be subject to k inequality constraints, so that the optimization problem may be expressed as:

$$\text{Minimize } f(X) = (f_1(X), f_2(X), \dots, f_n(X)) \quad (39)$$

$$\text{subject to } g_i(X) \leq 0 \quad \text{for } i = 1 \dots k$$

For this kind of problem, objectives typically conflict with each other. Thus, in most cases, it is impossible to obtain the global minimum at the same point for all objectives. Therefore, the problem has no single optimal solution but a set of efficient solutions representing the best objective "trade-offs". These solutions consist of all

design variable vectors for which the corresponding objective vectors cannot be improved in any dimension without improvement in another. They are known as Pareto-optimal solutions in reference to the famous economist. Mathematically, Pareto-optimality can be expressed in terms of Pareto dominance. Consider two vectors X and Y from the design variable space. Then, X is said to dominate Y if and only if:

$$\forall i \in 1..n \quad f_i(X) \leq f_i(Y) \quad (40)$$

$$\text{and } \exists j \in 1..n \Rightarrow f_j(X) < f_j(Y)$$

All design variable vectors which are not dominated by any other vector of a given set are called non-dominated regarding this set. The design variable vectors that are non-dominated over the entire search space are Pareto-optimal solutions and constitute the Pareto-optimal front.

B. Setting and Process of Optimization for “Passive” Wind Turbine System

In this section, the optimization of the “passive” wind turbine system which modelled on the section II is carried out using the NSGA-II. The design variables considered for the wind turbine optimization and their associated bounds are shown in Table II. Note that six variables are continuous (i.e. R_{rl} , R_{dr} , P_b , B_y , J_s and Ω_b) and two are discrete (i.e. p and N_{spp}). Two conflicting objectives have to be improved with respect to these variables: The useful power calculate as (36), has to be maximized while minimizing the total embedded mass of PMSG (reduced material and maintenance cost). The mass of PMSG is calculated by geometrical parameters on (27).

TABLE II. DESIGN VARIABLE RANGES FOR OPTIMIZATION

Design variable	Nature	Bounds
Bore radius/length ratio	Continuous	$R_{rl} \in [3, 6]$
Slot depth/ bore radius ratio	Continuous	$R_{dr} \in [0.2, 0.3]$
Current density	Continuous	$B_y \in [1.6, 1.8]$
Yoke induction	Continuous	$p \in \{10, \dots, 20\}$
Power at the base functional point	Continuous	$J_s \in [1, 3]$
Number of pole pair	Discrete	$P_b \in [10, 30]$
Number of slots per pole and phase	Discrete	$N_{spp} \in \{1, \dots, 3\}$
Base speed	Continuous	$\Omega_b \in [2.35, 6.25]$

The optimization also has to respect five constraints to ensure the PMSG feasibility in relation to the parametric variation of design variables in the optimization process.

The first two constraints (g_1 and g_2) concern the number N_{cs} of copper windings per slot, this number has to be higher than one and bounded by the slot section in relation to the minimum winding section $S_{winding}$ (this last is set to 0.5 mm²), g_3 concern the slot width w_s have to be larger than $w_{s_min}=10$ mm. The next constraint (g_4) prevents magnet demagnetization:

$$g_4 = \hat{B}_s - \hat{B}_g - B_D \leq 0 \quad (41)$$

An additional constraint (g_5) verifies that the temperature of the copper windings on steady-state (T_{bob})

does not exceed the critical limit of insulators (typically $T_{copper_max} = 180$ °C) during a wind cycle:

$$g_5 = T_{bob} - T_{copper_max} \leq 0 \quad (42)$$

The synoptic of the optimization process is displayed on Fig. 7. The optimization algorithm is coupled with the sizing and simulating models presented in the previous sections. The most accurate model, which can be used in an optimization process where multiple simulations are performed, is employed for simulating the wind turbine behavior.

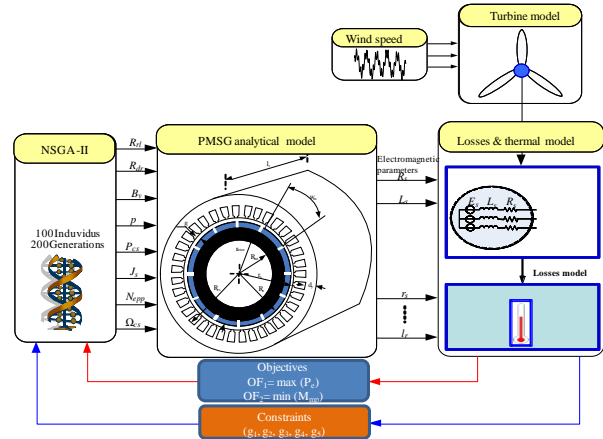


Figure 7. Process of optimization

IV. RESULTS AND DISCUSSION

A. Pareto's Front

To take into account the design constraints in the NSGA-II [15], the Pareto-dominance rule is modified as follows:

- If two individuals are non-feasible, the Pareto-dominance relative to these individuals is applied in the constraint space.
- If two individuals are feasible, the Pareto-dominance relative to these individuals is applied in the objective space.
- If one individual is feasible and the other non-feasible, the feasible individual dominates the non-feasible individual.

In this manner, Pareto ranking tournaments between individuals include the constraint as well as the objective minimization. Note that in the case of the NSGA-II, for non-feasible individuals belong to a given front in the constraint space, the computation of the I-distance density estimator is carried out in relation to all constraints [16]. In this way, niching will occur in the two different spaces (i.e. constraint and objective spaces) and diversity will be preserved to avoid premature convergence.

The population size and the number of non-dominated individuals in the archive are set to 100 and the number of generations is 200. Mutation and recombination operators are similar to those presented in [17]. They are used with a crossover probability of 1, a mutation rate on design variables of $1/m$ (m is the total number of design variables in the problem) and a mutation probability of

5% for the X-gene parameter used in the self-adaptive recombination scheme.

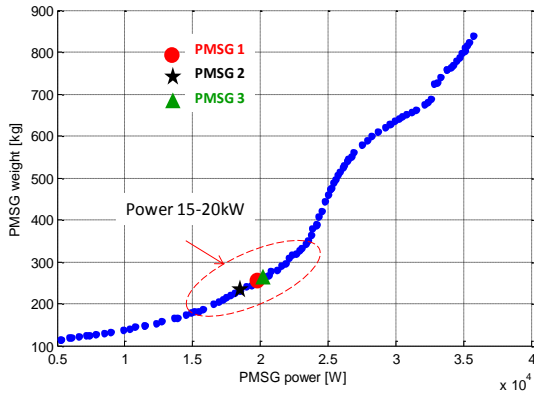


Figure 8. Pareto's front

Fig. 8 shows the Pareto's front of optimization process. We can see that the mass of PMSG is proportional of the useful power of system. As previous mention, the authors interest the PMSG on the area of 15-20kW. Then, three individuals PMSG1, PMSG2, PMSG3 are chosen for analysis the efficacy of optimized methodology. The detail parameters of three optimized PMSGs are presented on APPENDIX A.

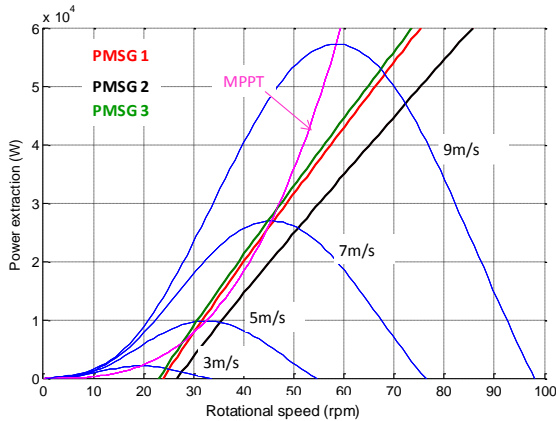


Figure 9. Extraction of PMSG power on plan of wind turbine power and wind speed

As it can be seen on Fig. 9, the power extraction of three solutions can match very closely the behavior of active wind turbine systems operating at optimal wind powers by using the MPPT control device. Particularly, on area of low wind speed from 4m/s to 8m/s, the power extractions of PMSG 1 and PMSG 3 are very near the MPPT extraction of wind turbine (the pink curve).

The extractions of torque of three optimized PMSG are shown on Fig. 10. We can consider that the torque extractions of PMSG1 and PMSG3 are seemly near the MPPT torque extraction of turbine.

The analysis results of power and torque of optimized motor on the characteristics of wind turbine justify that the efficiency of optimized methodology and confirm that by using the genetic algorithm, the system can be optimized to "natural" adaptation of wind turbine and PMSG in objective of power maximization. Furthermore, the power extraction of "passive" wind turbine system

can be comparative with the active structure controlled by MPPT strategy.

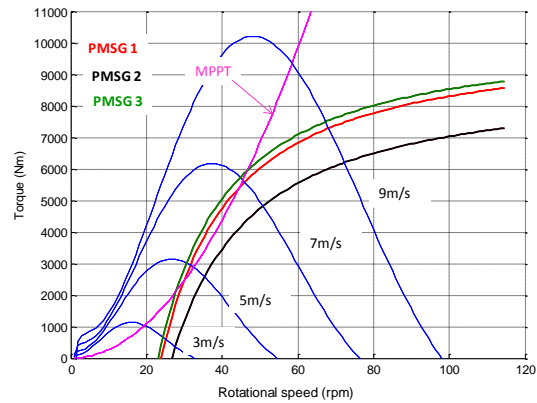


Figure 10. Extraction of PMSG torque on plan of wind turbine torque and wind speed

B. Simulation Results

In order to verification the dynamic behavior of "passive" wind turbine system. The optimized solution PMSG1 is simulated. In this simulation, the authors use the wind speed profile (1) during 30s and the simulation is established on Matlab/simulink environment. Fig. 11 presents the mechanical torque of wind turbine and the electromechanical torque of PMSG1. It seems that the similarity of the produced torque of turbine and captured torque of PMSG during the variation of wind speed.

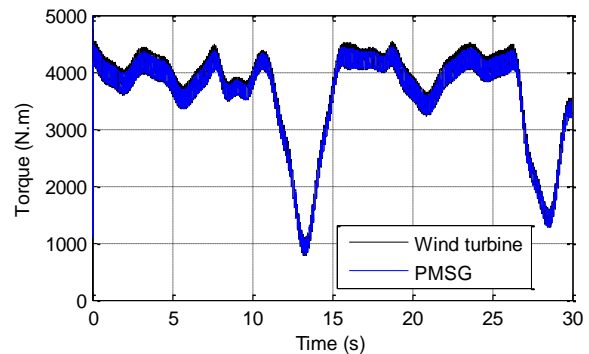


Figure 11. Wind turbine torque and PMSG1 torque

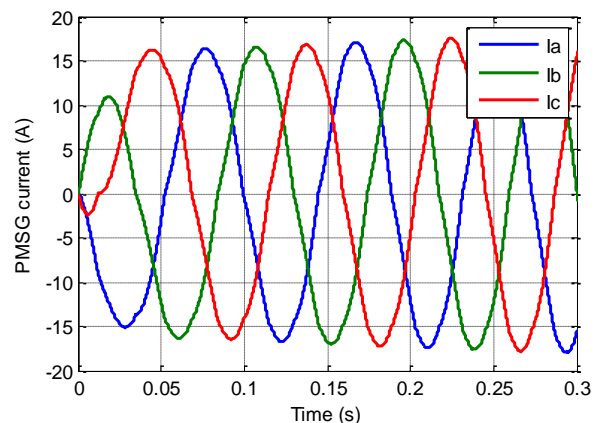


Figure 12. Phase currents of PMSG1

The zoom out of 300ms of phase current of PMSG1 is shown on Fig. 12 and the temperatures of PMSG1 are shown on Fig. 13, note that the evolution of temperature is depends the volume of generator, for PMSG1, this process is during about two hours and the temperature on steady-state calculate by (38) on the slot copper (T_{bob}) is 130 °C with the temperature of ambient air fix 25 °C on simulation.

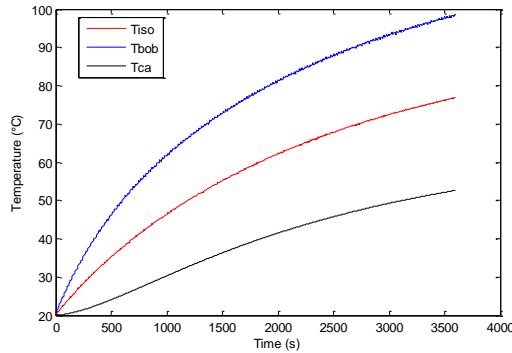


Figure 13. Evolution of temperature on stator of PMSG1

C. Optimized PMSG Geometric Behavior

The 3-D mechanical design of PMSG1 is presented on Fig. 14. Generally, to achieve assumed rated power 20kW at low wind speed (6m/s) there is a need to use low-speed PMSG [18]. It means a great number of poles in the rotor, and this in turn, introduces a high value of cogging torque. On Fig. 14, it is easy to see that the rotor of optimized PMSG1 has 40 poles, the active size of rotor is ($L \times D = 90 \text{ mm} \times 105 \text{ mm}$) and active the weight of PMSG1 is 254kg.

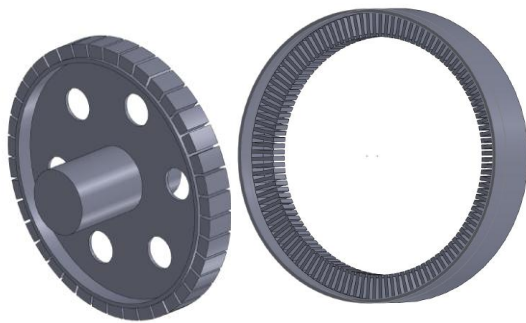


Figure 14. 3-D geometric model of PMSG1

V. CONCLUSION

The paper presents the methodology of design, optimization and analysis of PMSG for wind energy harvesting applications with the low average wind speed. The one without of power electronic and control (called “passive” wind turbine system) is the simplest structure on the wind turbine system. The “passive” wind turbine system does not need any sensors and control drives, is also the low-cost solution. On the other hand, the system is more robust with this architecture.

The efficiency of “passive” wind turbine system is taken by the optimization of PMSG according the natural adaptation of wind speed – turbine - PMSG. The authors

are designed the electromagnetic and electrothermal behavior of PMSG and used the genetic algorithm for optimization process. The results showed the significant improvement of the power extraction of “passive” wind turbine and the efficiency of methodology.

APPENDIX A OPTIMIZED PMSG PARAMETERS

Geometrical parameter	PMSG1	PMSG2	PMSG3
Bore radius (mm)	428	413	431
Air gap (mm)	10.5	10.5	10.5
Length active (mm)	90	83	90
Slot depth (mm)	87	82	87
Slot width (mm)	15	14.4	15
Tooth width (mm)	15	14.4	15
Rotor yoke thickness (mm)	13.2	12.7	13.3
Stator yoke thickness (mm)	13.2	12.7	13.3
Active weight (kg)	254	220	260
Number of pole pair	20	20	20
Number of slots per pole and phase	1	1	1
Electromagnetic parameters	PMSG1	PMSG2	PMSG3
Resistance (Ω)	2.56	2.643	2.663
Inductance (mH)	138	127	145
Flux (Wb)	7.24	6.48	7.50
Nominal torque (Nm)	4500	3900	5000
Nominal speed (rpm)	42.2	46.4	41.2
Nominal power (kW)	20	18.8	20

ACKNOWLEDGMENT

The authors wish to thank Hanoi University of Science and Technology (HUST) to finance support for this work in Renewable Energy Program of Vietnamese Government. This work was supported in part mechanical wind turbine design of mechanical department of HUST.

REFERENCES

- [1] D. S. Zinger and E. Muljadi, “Annualized wind energy improvement using variable speeds,” *IEEE Trans. Industry Application*, vol. 33, pp. 1444-1447, 1997.
- [2] O. Carlson, J. Hylander, and K. Thorborg, “Survey of variable speed operations of wind turbines,” in *Proc. Europ. Wind Energy Conf.*, 1996, pp. 406-409.
- [3] R. Cardenas, W. F. Ray, and G. M. Asher, “Switched reluctance generators for wind energy applications,” in *Proc. Power Elec. Specialist Conf.*, 1995, pp. 559-564.
- [4] E. Hau, *Wind Turbines*, Springer, 2000.
- [5] G. L. Johnson, “Wind energy systems,” Electronic Edition, December 2001.
- [6] Peter Vas, *Electrical machines and Drives- A Space Vector Theory Approach*, New York: Oxford University Press, 1992.
- [7] T. J. E. Miller, *Brushless Permanent-Magnet and Reluctance Motor Drives*, New York: Oxford University Press, 1989.
- [8] J. Ribrant and L. M. Bertling, Survey of Failures in Wind Power Systems With Focus on Swedish Wind Power Plants During 1997-2005.
- [9] G. Böhmeke, “Development and operational experience of the wind energy converter WWD-1,” in *Proc. Europ. Wind Energy Conf.*, 2003.
- [10] G. Slemon and X. Liu, “Modeling and design optimization of permanent magnet motors,” *Electrical Machines and Power Systems*, vol. 20, pp. 71-92, 1992.

- [11] P. H. Mellor, D. Roberts, and D. R. Turner, "Lumped parameter thermal model for electrical machines of TEFC design," in *IEE Proceedings B*, vol. 138, no. 5, 1991.
- [12] A. Boglietti, A. Cavagnino, M. Lazzari, and M. Pastorelli, "A simplified thermal model for variable speed self cooled industrial induction motor," *IEEE IAS Annual Meeting Conf. Rec.*, Pittsburgh, USA, 13-17 October 2002.
- [13] B. Sareni, A. Abdelli., X. Roboam, and D. H. Tran, "Model simplification and optimization of a passive wind turbine generator," *Renewable Energy*, vol. 34, no. 12, pp. 2640-2650, 2009.
- [14] Deb, S. Agrawal, A. Pratab, and T. Meyarivan, "A fast-elitist non-dominated sorting genetic algorithm for multiobjective optimization: NSGA-II," in *Proc. Parallel Problem Solving from Nature VI Conference*, 2000, pp. 849-858.
- [15] K. Deb, S. Agrawal, A. Pratab, and T. Meyarivan, "A fast-elitist non-dominated sorting genetic algorithm for multiobjective optimization: NSGA-II," in *Proc. Parallel Problem Solving from Nature VI Conference*, Athens, Greece, 2000, pp. 849-858.
- [16] B. Sareni, J. Regnier, and X. Roboam, "Integrated optimal design of heterogeneous electrical energetic systems using multiobjective genetic algorithms," *International Review of Electrical Engineering*, vol. 1, no. 1, pp. 112-129, 2006.
- [17] B. Sareni, J. Regnier, and X. Roboam, "Recombination and self-adaptation in multi-objective genetic algorithms," *Lecture Notes in Computer Science*, vol. 2936, pp. 115-126, 2004.
- [18] Z. Goryca, M. Ziółek, and M. Malinowski, "Cogging torque of the multipolar generator with permanent magnets," *Maszyny Elektryczne Zeszyty Problemowe*, vol. 88, 2010.



The-Cong Nguyen was born in Hanoi, Vietnam, in 1957. He received the DEA on Juin 1991 then Ph.D. on September 1994 in electrical engineering in Laboratoire d'Electrotechnique de Grenoble (LEG) of

Institut National Polytechnique de Grenoble (INPG), France.

From 1980 till now, he is lecturer for the courses: electrotechnic, power electronic and drive motor at School of Electrical Engineering (SEE) - Hanoi University of Science and Technology (HUST), Hanoi, Vietnam. His current research's direction is the electrical machines as linear induction motor, the renewable energy dedicated to wind and photovoltaic energy.



Duc-Hoan Tran was born in Nam Dinh, Vietnam, in 1983. He received the M.Sc. and Ph.D. in electrical engineering from Institut National Polytechnique de Toulouse (INPT), Toulouse, France on Juin 2007 and September 2010, respectively.

From 2010 to 2012, he was working toward the post-doctoral degree at the Laboratory of Plasma and Energy Conversion, National Center of Scientific Research INPT-UPS, Toulouse, France. In 2013, he joined at the Department of Power Electronics and Control - ALTRAN Technology in Toulouse, FRANCE, where he is currently an engineer R&D in aeronautic engineering.

His research interests include the design of power systems dedicated to wind turbines and power energy conversion, optimization algorithms, electro-mechanic conversion, power electronics and control design.



Thanh-Khang Nguyen was born in Thanh Hoa, Vietnam, in 1984. He received BE and ME degree in electrical engineering from Hanoi University of Science and Technology (HUST) in 2007 and 2010, respectively. He is currently a Ph.D. student at Hanoi University of Science and Technology.

His research interests include photovoltaic, wind power system and power electronic converter.